

Electric Waterjet Thruster Vessel Development – Concept, Charger, and Battery Monitoring

Kin Lung Jerry Kan¹, Y.C. FONG², IP Shu Chuen³, H.K.T. Tsang⁴, H.F. Ho⁵, X.D. Xue⁶, Y.L. Fan⁷, K.W.E. Cheng⁸

Power Electronics Research Centre, The Hong Kong Polytechnic University, Hong Kong

¹E-mail: jerry.kan@connect.polyu.hk, ²E-mail: yat-chi.fong@polyu.edu.hk, ³E-mail: shu.ip@polyu.edu.hk,

⁴E-mail: hon-ki.tsang@polyu.edu.hk, ⁵E-mail: james.ho@polyu.edu.hk, ⁶E-mail: xd.xue@polyu.edu.hk,

⁷E-mail: yulong.fan@polyu.edu.hk, ⁸E-mail: eric-cheng.cheng@polyu.edu.hk.

Abstract— This paper exhibits an overall design of an electric waterjet vessel. Marine craft electrification especially the propulsion system transfer from the diesel engine to electric switched reluctance motor realizes the environmental-friendly utilization. A corresponding waterproof inductive wireless charger which could operate under water-immersed condition is introduced to prompt higher marine craft electrical penetration. This work presents the first development of a novel design of a marine charging system on a jet boat environment for lower power application. The use of near field magnetic transfer lifts the power conversion efficiency and at the same time, improves the safety and reliability of the charging operation. The system has been built and tested successfully to validate the concept boat.

Keywords— Marine electrification, Waterproof inductive charger, switched reluctance motor-driven waterjet.

I. INTRODUCTION

Ideally the diesel engines have high fuel energy density which is almost 181g fuel/kWh that suits the transportation application well. However, the vessels have various operation mode. The standby mode and relocation a boat is on boarding progress representing an extreme low load condition which drags the fossil fuel generator performance [1]. Furthermore, the motor driven propeller and waterjet bow thruster propulsion system enable the regenerative braking and energy generation which boosts the system efficiency. The e-ferry energy cost performance 0.11\$/kWh has 13 times higher than the diesel engine around 1.38\$/kWh upon the entire service scenarios [2].

The diesel combustion engine emission problems bring great concern on the environmental protection. International Marine Organisation (IMO) posed restricts on the exhaust emission value of oxides of nitrogen. For the engine maximum operation speed (n/rpm) over 2000, the NO_x emissions limits should be 1.96g/kWh from 2016 at the NO_x emission-controlled area (ECA) and globally 7.7g/kWh. The sulphur limit value is 0.1% (m/m) in SO_x-ECA while the corresponding content is 0.5% (m/m) on global from 2020 [3]. Obviously there are three methods: 1. retire the unqualified craft, 2. replace or improve the diesel engine on existing boat, 3. implement the new generation vessel such as e-ferry driven by battery which is exhaust emission free. In addition, there are oil residue, operation noise to ambient environment comprises of onshore and underwater. Flaws result in numerous ecology catastrophe. Dylejko presented the total radiated noise levels of marine diesel engines with different vibration isolation system maintain from 98dB to

140dB under 1kHz [4]. 2016, US National Marine Fisheries Service (NOAA) issued a marine mammal guidance to regulate the vessel acoustic thresholds by marine mammal auditory weighting function. The non-impulsive receiving level of the ferry should be 120dB and impulsive is 160dB [5]. Fig. 1 reveals, in light of the relative silent operation motor and the intrinsic enclosure impeller structure, battery-motor-driven waterjet propulsion system mitigates the load noise, marine fauna amputations cause by propeller [6] and the complicated combustion engine ducts mechanism.

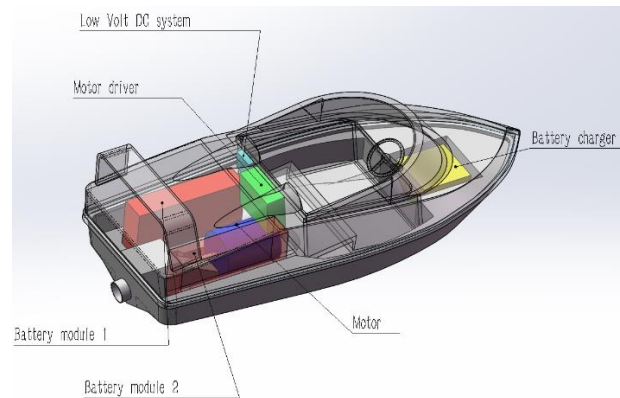


Fig.1 Propulsion system profile

The conventional e-ferry battery charging method is conductive charging with a metal plug. However, coastal ferries operate outdoor and always in a harsh and saline environment which challenges electrical safety. In the latest marine wireless charging application, there is a 1-MW inductive charging system in Norway [7]. The fixed installation makes it only suit the regular route cruise and the harbour with high power capacity. In a wide fjord area, the power grid is not strong. A pre-charged power dock consisted of the battery is an alternative method for high power transfer which can provide a 20-min fast charge [7]. But the expense of battery limits the e-ferry transportation cover area. High mobility and a user-friendly charger would be essential for the mass electrification of small vessels. An all insulated, small in size and 13-A socket applicable wireless charger is in desire.

This paper presents the propulsion, control, and energy storage system electrification. Section II introduces the propulsion system of the waterjet engine including the battery, motor, and waterjet characteristics. A magnetic-based all-insulated inductive wireless charger is illustrated

in section III. In section IV, the onboard DC distribution is presented briefly. Section V exhibits the experiments to validates the proposed concept.

II. PROPULSION SYSTEM & BATTERY

1. Waterjet pump operation profile

Pumps of waterjet are classified as axial flow, mixed flow, and centrifugal flow pumps for the angles of inflow and outflow [8]. Fig.2 reveals a common and typical mixed flow impeller pump for the waterjet engine. The waterjet engine propulsion system is composed of the inlet duct, impeller, driveshaft, stator, and nozzle. The rotating impeller driven by the shaft generates the thrust to provide the propulsion force with a directional control nozzle. Driveshaft coupled with the switched reluctance motor (SRM) in this case. SRM is very suitable for the marine and ship application for high operation performance [9]. Propulsion force provided by the waterjet engine is decided by the mass flow experienced in the impeller and the water leave velocity from the nozzle:

$$\dot{m} = \rho A_2 V_2 \quad (1)$$

where ρ is the sea water density, A_2 is the outlet duct area. Hence, the thrust T could be acquired by the rate of the water momentum changes through the nozzle, and the propulsion power P_p is:

$$T = \dot{m}(V_2 - V_1) = \rho A_2 V_2 (V_2 - V_1) \quad (2)$$

$$P_p = TV_S \quad (3)$$

The propulsive performance η_D could be determined by the cascaded efficiency formula [10]:

$$\eta_D = \eta_H \eta_O \eta_R \eta_C \eta_M \quad (4)$$

where η_H is the hull efficiency which indicates the power transfer from all propulsors to the hull traction power. η_O exhibits thrust power performance of the impellers. The impeller operation efficiency varies from the open water condition to actual condition that η_R is given to amend it. η_C, η_M are the shaft coupler efficiency and the motor efficiency.

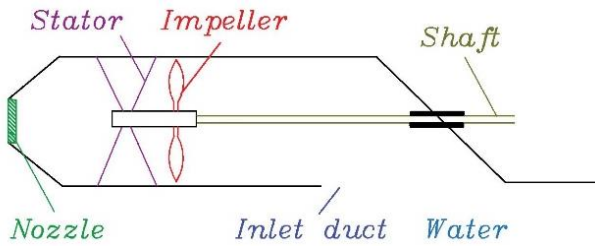


Fig.2 Waterjet thruster structure

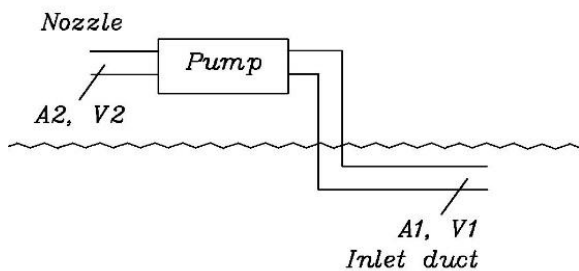


Fig.3 Idealized waterjet thruster arrangement

2. Switced reluctance motor designing

The SRM installation conducted as Fig.4. compared with the fossil fuel engine, it is more silent to drive and reduces the vibration caused residual resistance and skin friction resistance. There is a trade-off between the high power and less weight of the motor. Less weight eases the immersive of the hull which reduces much resistance. Fig.5 proposes an SRM design flowchart.

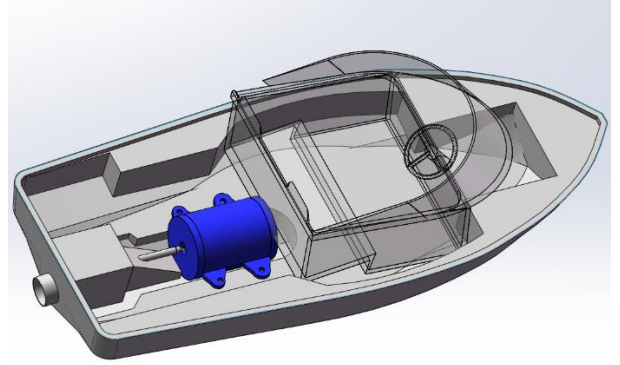


Fig.4 SRM installation position.

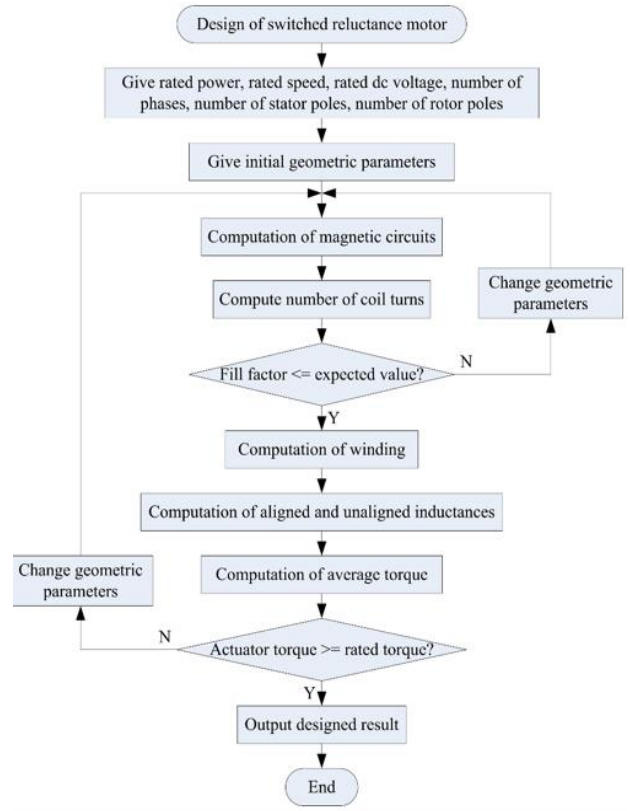


Fig.5 SRM design flow chart.

3. Lithium ion phosphate battery

Though the Lithium-ion phosphate (LFP) battery has approximately 10-30% energy density lower than the other lithium battery, the concern of safety and environment makes it a suitable choice. LFP is a cobalt-free Lithium battery, it reduces the pollution to the environment even battery sunk to the water. The difficulty in the ignition even at charging or short circuit circumstances make it a feasible power source on board.

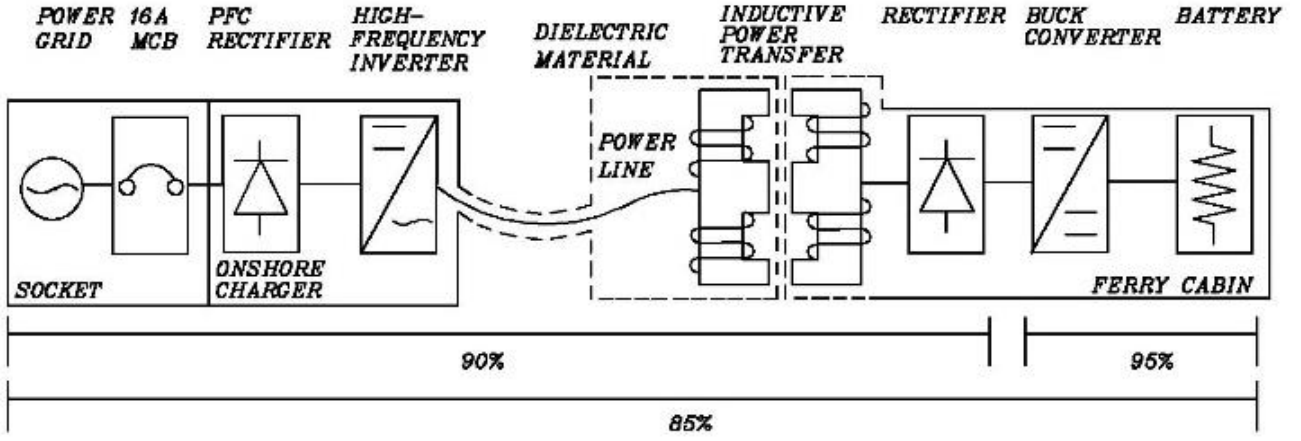


Fig.6 A standard LLC WPT system with 85% overall efficiency

III. ALL INSULATED WIRELESS CHARGER

Inductive power transfer through the time-vary magnetic field guarantees a high-efficiency wireless power transfer. A well-insulated coil generates a high-frequency magnetic field for vessel battery charging does not have any electric shock hazard to the creature. Both transmitter and receiver of the charging system covered by dielectric material prevent the potential risk of conductive charging with metal contacts.

LLC resonance circuit offers a high efficiency inverting technique for wireless charging. Fig.7 is a typical LLC converter topology and the transformer Tx could be primary and secondary side separated to form the metal-free power transfer. The primary side acts as a transmitter while the secondary side performs as a receiver. The merit of LLC circuit is the zero-voltage switching (ZVS). The concept is that before the switch turns on, the reverse diode conducts so that the switching voltage is set as the diode forward voltage which should be a relatively low value. The key measure is to set the switching frequency in the vicinity of the resonance frequency:

$$f_0 = \frac{1}{2\pi\sqrt{L_r C_r}} \quad (5)$$

$$f_n = \frac{f_{sw}}{f_0} \quad (6)$$

The loop inductance and the leakage inductance of the charging loop constitute the resonance inductance L_r . A capacitor C_r is deployed to generate the alternative current from DC in the full-bridge circuit. First Harmonics Approximation (FHA) is an effective way to estimate and design the circuit parameter. V_{oe} is the equivalent output voltage of the LLC circuit. L_m is the magnetizing inductance between the WPT transmitter and hull receiver while L_r represents the resonant inductance of wire parasitic inductance, transformer leakage inductance and power line loop inductance. C_r is the compensation capacitor.

$$V_{oe} = \frac{2V_{DC}\sin(2\pi f_{sw}t)}{\pi} \quad (7)$$

$$V_{oe_rms} = \frac{V_{in}}{\pi\sqrt{2}} \quad (8)$$

$$I_{oe_rms} = \frac{\pi I_o}{n2\sqrt{2}} \quad (9)$$

$$R_e = \frac{V_{oe_rms}}{I_{oe_rms}} = \frac{8n^2}{\pi^2} R_{load} \quad (10)$$

Therefore, the equivalent quality factor Q_e could be estimated:

$$Q_e = \sqrt{\frac{L_r}{C_r}} \quad (11)$$

$$M_g = \frac{V_{oe}}{V_{ge}} = \left| \frac{jX_{Lm} \parallel R_e}{(jX_{Lm} \parallel R_e) + j(X_{Lr} - X_{Cr})} \right|$$

$$= \left| \frac{L_n f_n^2}{[(L_n + 1)f_n^2 - 1] + j[(f_n^2 - 1)f_n Q_e L_n]} \right| \quad (12)$$

$$V_o = \frac{M_g V_{in}}{n} \quad (13)$$

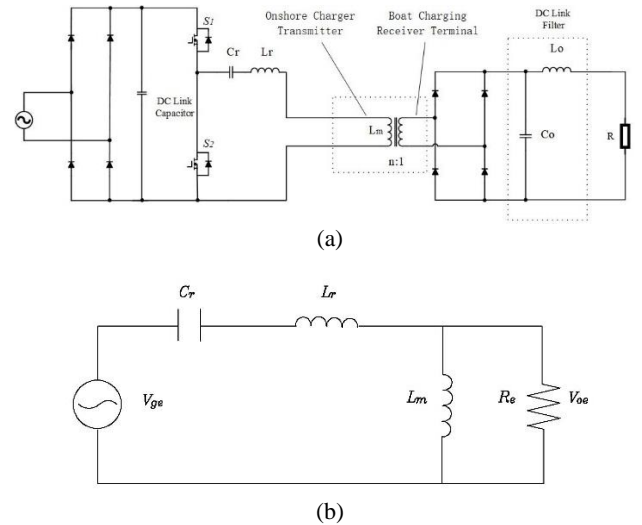


Fig.7(a) LLC circuit configuration;(b) FHA model

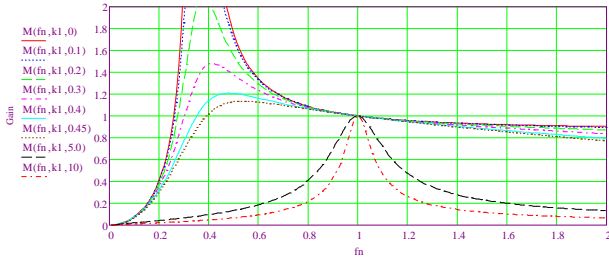


Fig.8 M_g Circuit gain curve

At the conventional LLC converter, one advantage is frequency modulation but not in wireless power transfer (WPT) application. Due to the low-quality factor the WPT configuration, the M_g , LLC converter gain curve with switching frequency varies drastically. Circuit gain changes intensively to maintain a steady output voltage. In Fig.5, the Q_e curves from 0.1 to 0.45 show extremely sharp which is not in compliance with the effective circuit gain control. It is preferred to set at one fix inverter operation switching frequency for power transfer. As to the charging power regulation, a DC/DC converter, for example, a buck converter should be applied to control the output voltage and current level. Constant current (CC) and constant voltage (CV) charging strategy adopted in this prototype. At last, due to the Q_e changes with load, that floats the circuit gain and output voltage. Hence, the full-load no-load output voltage range control should be done prior to circuit design.

IV. ELECTRIC VESSEL DC DISTRIBUTION SYSTEM

Hierarchical control is designed to decouple behaviour between different layers. This improves the over safety of the system [11]. Thereby the proposed network reveals in Fig.9. Battery regulated by a main bidirectional DC/DC converter is useful for the optimal real-time voltage and current of droop characteristics [12]. As mentioned, the busbar voltage level is 150V while the user interface voltage is 36V. The SRM motor signal including the speed, voltage and current data would be recorded by the VCU and to estimate the hull velocity and power consumption with reference of the battery SoC revealing on the panel. The battery regulation converter would be the primary protection of the battery for the unexpected overvoltage from the motor or the insulation fail in the network. The secondary protection is conducted by each inverter or DC/DC converter to cur the fault if overcurrent occurs.

TABLE 1: E-vessel parameter

Hull material	Glass fibre
Capacity	2-person
Rated velocity	18knots
Maximum velocity	26knots
Waterjet type	Mixed flow impeller
Motor type	Switched Reluctance Motor
Motor nominal power	20kW
Motor maximum power	55kW
Power source	LFP battery
Battery voltage range	300V/80Ah
User interface voltage	36V
Busbar voltage	150V

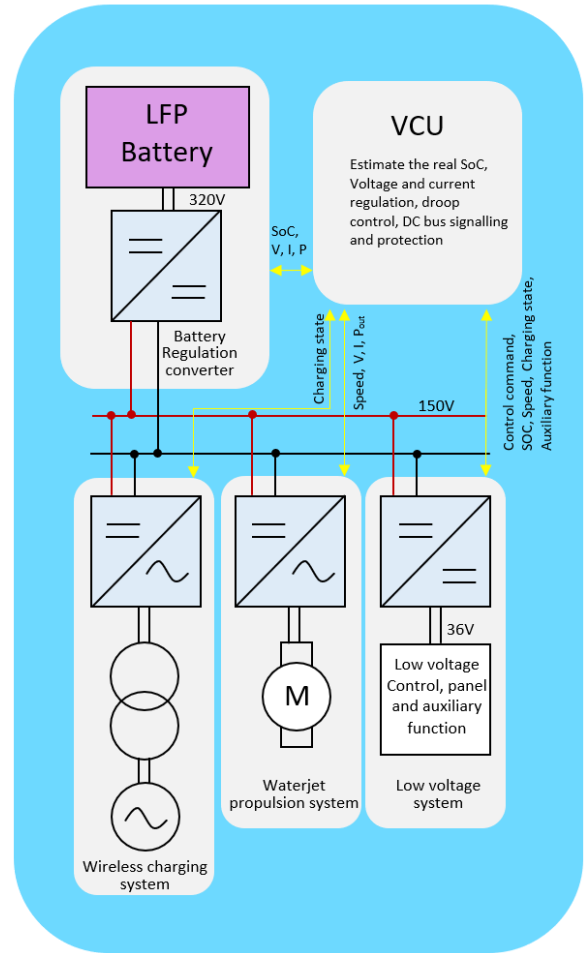


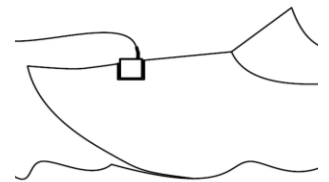
Fig. 9 The proposed DC distribution network for small e-vessel

V. SIMULATION AND EXPERIMENT RESULT

A 1.4kW all insulated inductive wireless charger prototype has been developed to validate the proposed concept. Fig. 10(a) reveals the live coil, ferrite and thermal detector are immersed into the epoxy until to be an integrated structure with the shell. A 9.42mm sq. litz wire implemented to ease the skin effect of charger high frequency operation and avoid the high temperature for the enclose of wire from air. The powerline extended from the charger box to the coil plug is protected by a grounded armoured tube in case of any potential mechanical destroy at the charging spot. Mobile charger transmitter plug was designed with a handle to be plugged on the receiver. The top-edge of the cupped receiver should be fixed on the surface. All the exposure components are water-resistance.



(a)



(b)

Fig. 10 (a)Transparent demonstration for the concept of all insulated WPT charger covered by epoxy. (b)Charging scenario.



(a) (b)
Fig.11 The all-insulated inductive charger

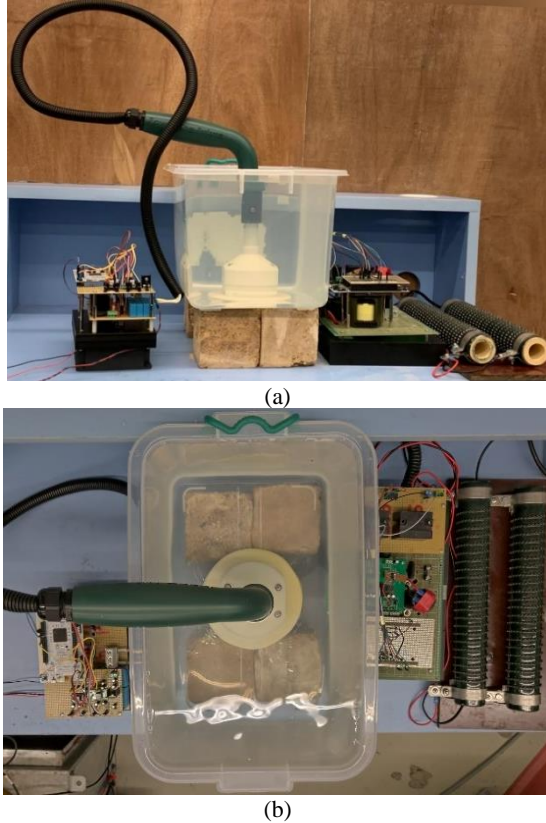


Fig.12 The proposed all insulated charger tested in water tank
(a) front view;(b) top view.

TABLE 2: E-vessel contactless charging system parameter	
LLC WPT Charger	
Maximum Power	1.4kW
Input voltage	220V AC
Power line current	13.5A
Receiver input voltage	232V AC
Operation frequency	145kHz
Regulation Buck Converter	
Battery side voltage range	200V to 400V DC
Busbar side voltage range	90V to 153V DC
rated current	8A
Overall system	
Full power operation efficiency	89.3%

As the DC distribution Fig.13, the regulation DC/DC buck converter is connected to the 150 V DC busbar. The charging experiment formed as Fig.12 and the 20 Ω resistance was used to emulate the charging current to the

battery. The result indicating on Fig.13(A) shows the drain-source voltage of S4 in Fig.6(a) Resonance current I_r is negative at the moment of S4 is turning on. ZVS achieved owing to the small forward voltage of reverse-diode. Fig.13(b) releases the LLC WPT circuit characteristics of two-port network under full load circumstance which means the starting point of CV charging. The maximum operation efficiency of the LLC WPT charger is 92.6% with 1.4kW input power with sufficient ventilation in the charging box. Fig.14 is the regulation buck converter profile and the power flow from charger to battery management system circuit is 150V busbar DC voltage with 8A charging current.

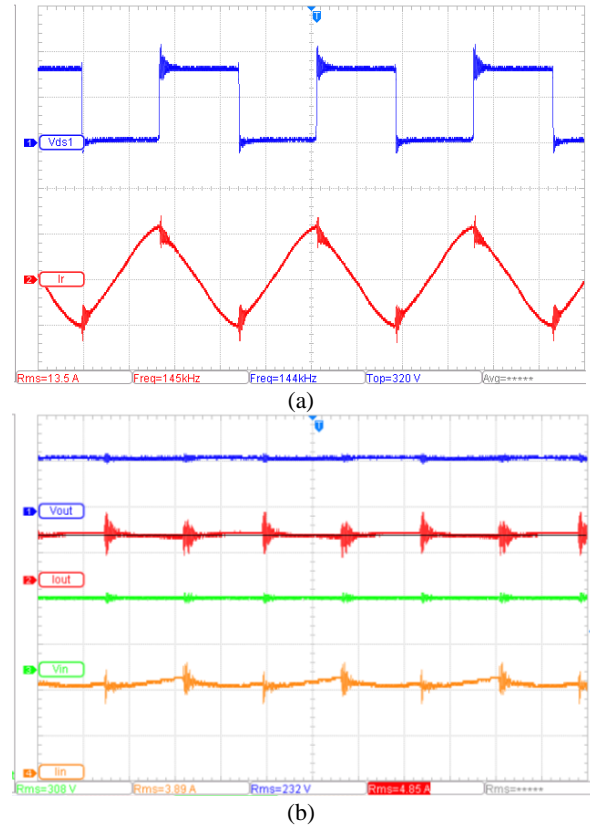


Fig.13 (a)ZVS of the full bridge test rig: CH1,S4 MOSFET drain source voltage; CH2, current in power line. (b)Full-load operation. CH1,Output voltage: V_{out_LLC} (200v/div); CH2,output current: I_{out_LLC} (5A/div); CH3,input voltage: V_{in} (200V/div); CH4,input current I_{in} (2A/div);

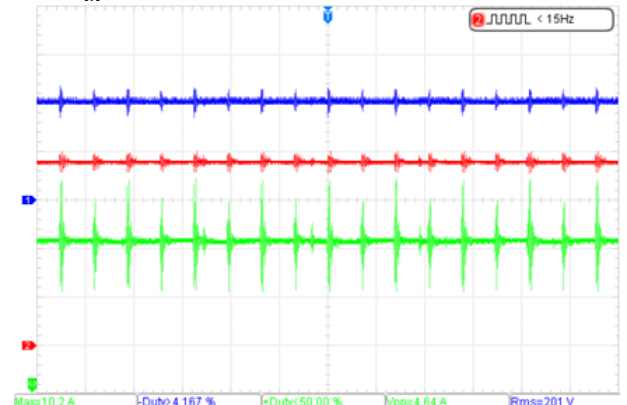


Fig.14, Charging system comprise with the receiver buck converter full power constant voltage charging waveform:CH1,input voltage: V_{out_LLC} (100v/div); CH2,output voltage: $V_{out_DC busbar}$ (40v/div); CH3,output current: I_{out} (2A/div),8A RMS.

A simulation study was conducted to investigate the battery behaviour during sailing. The 300V LFP module was developed based on the study presented in [13]. At various capacities ranged from 40Ah to 80Ah, the SOC as well as the bus voltage profile of the battery pack under loading at different C-rates and constant power of 20kW has been simulated in Fig.15.(a). As shown in Fig.15, the voltage and SOC curves for the case of (2), (5), (8) and (3), (6), (9) at the 1C and 2C discharging rates are overlapped together, which are fully discharged after 1800s and 3600s, respectively. Considering the cases of 20kW constant power discharge, with a 40Ah battery pack, the battery took about 2100s to discharge from the initial voltage of about 312 V to 290 V, whereas when the capacity was double to 80Ah, or approximately 24kWh, the battery pack lasted for more than 4300s. It could also be noted that with large battery size, the case of 80Ah had the lowest initial voltage drop of about 3 V. This implies that the lowest internal resistance could help improve the energy efficiency as well as the performance of the SRM motor drive. This gives a preliminary estimation of the required battery size given the constraints in space and weight available in the vessel design.

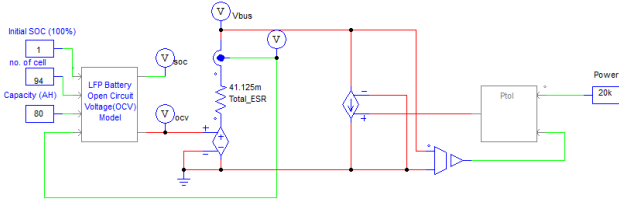
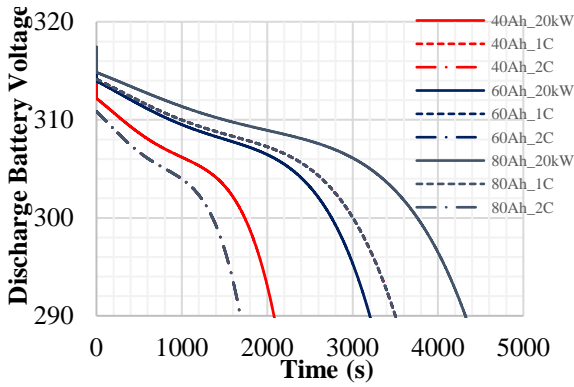
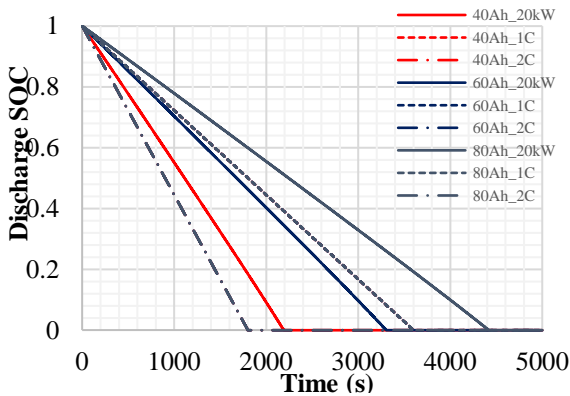


Fig.14 Battery discharging simulation schematics



(a)



(b)

Fig.15 (a)Discharging battery voltage at different discharging current. (b)Discharging SOC at different discharging current.

TABLE 3: Design specification of battery module for electric vessel

Parameter	Value
Battery type	LiFePO4(LFP)
Nominal cell voltage	3.2V
Capacity	300V/80AH
Battery voltage range	290V to 312V
Charging cycle	>1000
Maximum discharging	150A
Casing	Stainless stell
IP rating	IP67
Module weight	140kg
Dimension	450*930*170 mm

VI. CONCLUSION AND FUTURE WORKS

This paper provides an electrification solution for a small waterjet engine vessel. A rigid and all insulated inductive wireless charger has been proposed to cater to the safer utilization and higher mobility of the mass on marine electrification. The wireless power transfer concept is adopted in the charging system but it is based on near flux power transfer. The top efficiency of the charger is 89.3% that is considered to be high for the subject. The coil and core are covered by the plastic shell and epoxy filler so that there is no metal or live component accessible. The LFP battery discharge simulation was conducted to validate the concept feasibility and high-efficiency operation. A vessel-based DC distribution system of 150V to power up the whole vessel is designed. All the components of a charger, motor drive, battery management, and control have been integrated into the e-vessel.

The future works include conducting a power test of the waterjet engine driven by SRM, to investigate the range speed and cruise speed. Development of a control algorithm of motor speed, torque relationship corresponding to the waterjet pressure head, mass flow to decrease the power density of the propulsion system for a higher speed. Considered the environmental protection, not only the assembly and integrated with flexible photovoltaic panels, even to explore the possibility of an unmanned marine vehicle is driven offshore PV generating field. It would be interesting to make the mobile generator and power bank based on E-vessel come reality.

ACKNOWLEDGMENT

The authors wish to acknowledge the support of the Innovation and Technology Funds under the project code ITS/073/18FP and the support provided by the members of the Power Electronics Research Centre (PERC), Department of Electrical Engineering, The Hong Kong Polytechnic University.

REFERENCES

- [1] O. L. Osen, "Optimizing electric energy production on-board offshore vessels: Vessel power consumption profile and production strategies using genetic algorithms," OCEANS 2016 - Shanghai, Shanghai, 2016, pp. 1-10, doi: 10.1109/OCEANSAP.2016.7485614.
- [2] K. W. E. Cheng, X. D. Xue and K. H. Chan, "Zero emission electric vessel development," 2015 6th International Conference on Power

Electronics Systems and Applications (PESA), Hong Kong, 2015, pp. 1-5, doi: 10.1109/PESA.2015.7398965.

- [3] International Convention for the Prevention of Pollution from Ships, 1973 as modified by the Protocol of 1978(MARPOL 73/78), International Maritime Organization, 1978.
- [4] Jianping Bi, Xinli Wang and Lili Li, "Diesel noise measurement and control of behavior analysis," 2011 Second International Conference on Mechanic Automation and Control Engineering, Hohhot, 2011, pp. 5730-5732, doi: 10.1109/MACE.2011.5988332.
- [5] National Marine Fisheries Service, "Technical Guidance for Assessing the Effects of Anthropogenic Sound on Marine Mammal Hearing: Underwater Acoustic Thresholds for Onset of Permanent and Temporary Threshold Shifts," 2016.
- [6] Roger W. Byard, Calle Winskog, Aaron Machado, Wayne Boardman, "The assessment of lethal propeller strike injuries in sea mammals, " *Journal of Forensic and Legal Medicine*, Marine pollution bulletin, Vol.153, p.111031-111031, 2020-04.
- [7] G. Guidi, J. A. Suul, F. Jensen and I. Sorfonn, "Wireless Charging for Ships: High-Power Inductive Charging for Battery Electric and Plug-In Hybrid Vessels," in *IEEE Electrification Magazine*, vol. 5, no. 3, pp. 22-32, Sept. 2017, doi: 10.1109/MELE.2017.2718829.
- [8] Arash Eslamdoost, "Investigations of waterjet/hull interaction effects," Ph.D. Thesis, Department of Shipping and Marine Technology, Chalmers University Of Technology, Gothenburg, Sweden, 2012
- [9] S. Elsaiah and C. Brady-Alvarez, "A Switched Reluctance Motor Drive System for Future Applications in the Emerged IMPS," 2018 North American Power Symposium (NAPS), Fargo, ND, 2018, pp. 1-5, doi: 10.1109/NAPS.2018.8600583.
- [10] D Stapersma, Hk Woud, "Matching propulsion engine with propulsor," *Journal of Marine Engineering & Technology*, 4:2,pp. 25-32, 2005
- [11] Z. Jin, G. Sulligoi, R. Cuzner, L. Meng, J. C. Vasquez and J. M. Guerrero, "Next-Generation Shipboard DC Power System: Introduction Smart Grid and dc Microgrid Technologies into Maritime Electrical Networks," in *IEEE Electrification Magazine*, vol. 4, no. 2, pp. 45-57, June 2016, doi: 10.1109/MELE.2016.2544203.
- [12] Y. C. Fong, K. W. E. Cheng and R. Sekhar, "A Current Allocation Strategy Based Balancing Technique of Voltage Source String in Switch-Ladder Inverter and Its Switched-Capacitor Variety," in *IEEE Transactions on Energy Conversion*, doi: 10.1109/TEC.2020.3031224.
- [13] Caihao Weng, Jing Sun and Hui Peng, ""A Current Allocation Strategy Based Balancing Technique of Voltage Source String in Switch-Ladder Inverter and Its Switched-Capacitor Variety," in *IEEE Transactions on Energy Conversion*," in dynamic systems and control conference, 2014